Available online at www.sciencedirect.com
SCIENCE DIRECT®

Thermochimica Acta 435 (2005) 92–98

thermochimica acta

www.elsevier.com/locate/tca

Thermal analysis and spectroscopic characteristics of tetrabutylammonium tetrachloroferrate(III)

Dariusz Wyrzykowski [a], Tomasz Maniecki [b], Agnieszka Pattek-Janczyk [c], Jan Stanek [d], Zygmunt Warnke [a,*]

[a] *Faculty of Chemistry, University of Gdańsk, Sobieskiego 18, 80-952 Gdańsk, Poland*
[b] *Institute of General and Ecological Chemistry, Technical University of Łódź, Żwirki 36, 90-924 Łódź, Poland*
[c] *Faculty of Chemistry, Jagiellonian University, Ingardena 3, 30-060 Kraków, Poland*
[d] *M. Smoluchowski Institute of Physics, Jagiellonian University, Reymonta 4, 30-059 Kraków, Poland*

Received 24 February 2005; received in revised form 27 April 2005; accepted 4 May 2005
Available online 16 June 2005

Abstract

The IR, far-IR, Raman and Mössbauer spectra have been utilized to identify a new compound consisting of a tetrachloroferrate(III) anion and a tetrabutylammonium cation $[(C_4H_9)_4N][FeCl_4]$. Its degradation has been studied by thermal analysis using TG, TG–MS, DTG and DTA, as well as DSC techniques. The measurements were run in static air and in argon atmosphere. Solid residues were identified by elemental analysis, far-IR and Mössbauer spectroscopy. The discussion was focused on processes proceeding during the first step of the thermal decomposition.

Keywords: Tetrachloroferrate(III); Thermal decomposition; IR; Raman; Mössbauer spectroscopy

---

1. Introduction

A number of complexes with a tetrahedral tetrachloroferrate(III) anion have been reported. Crystal structures of some of these compounds have been established by X-ray crystallography. The mean weighted Fe–Cl bond lengths and the Cl–Fe–Cl angles found in the Cambridge Structural Database version 5.25, November 2003, are 2.204 Å and 109.32°, respectively, for the non-associated $[FeCl_4]^-$ ion (a total of 164 structures). Investigation of this ion have also been confined to its magnetic [1,2] and spectroscopic [3–5] features, and more recently, to its interaction with non-aqueous solvents [6,7]. However, thermal properties of the tetrachloroferrates(III) have not been studied so far. For this reason, it seemed worthwhile to carry out research on just this subject. This contribution initiates a series of efforts confined to the study of thermal decomposition of complexes consisting of mono $[FeX_4]^-$, and mixed $[FeX_{4-n}Y_n]^-$ (X, Y = Br or Cl; $n = 0, 1, 3, 4$), tetrahalogenoferrate(III) anions and nitrogen-containing organic bases as cations.

Now we are presenting the synthesis, spectroscopic characteristics (IR, Raman, Mössbauer) and results of thermal analysis (TG, TG–MS, DTG, DTA and DSC) of a new salt, tetrabutylammonium tetrachloroferrate(III).

2. Experimental

2.1. Synthesis and chemical analysis

The title compound, $[(C_4H_9)_4N][FeCl_4]$, was synthesized by a method similar to that previously used by us for obtaining other tetrachloroferrates(III) [7]. Thus, an ethanolic solution of ferric chloride (Aldrich) was prepared by dissolving 0.03 mol of $FeCl_3$ in absolute ethanol and a stoichiometric quantity of an ethanolic solution of tetrabutylammonium chloride (Aldrich) was added to it. Immediately after mixing the solutions an amorphous yellow precipitate

---

* Corresponding author. Tel.: +48 58 3450366; fax: +48 58 3410357.
E-mail address: warnke@chem.univ.gda.pl (Z. Warnke).

0040-6031/$ – see front matter © 2005 Elsevier B.V. All rights reserved.
doi:10.1016/j.tca.2005.05.007

of $[(C_4H_9)_4N][FeCl_4]$ fell out. It was recrystallized from ethanol, washed with an ethanol–ether (1:1) mixture and dried in a vacuum desiccator over P_4O_{10}. When the synthesis was carried out in water, the compound crystallized out only after a few days. The identity of the compound was confirmed by elemental analysis (C, H, N) and potentiometric titration of the chloride with a standardized 0.1 M solution of $AgNO_3$.

2.2. Instrumental

Potentiometric titrations were carried out using standard electrodes, SCE (indicator electrode) and silver electrode (the reference one). The IR spectra were recorded on a BRUKER IFS 66 spectrophotometer in a KBr pellet over the 4400–650 cm^{-1} range and the far-IR spectra (650–50 cm^{-1} range) were taken in PE. The Raman spectra were recorded on a BRUKER FRA 106 spectrophotometer.

The Mössbauer spectra were recorded at room (293 K) and low (90 and 220 K) temperatures by means of conventional spectrometer in transmission geometry using a ^{57}Co/Rh source. A gas flow cryostat was applied for low temperature measurements. The samples were prepared in pellets with thickness of ca.10 mg Fe/cm^2. The spectra were numerically analysed by a least-squares procedure assuming Lorentzian line shapes and isomer shifts are quoted relative to α-Fe.

Thermogravimetric measurements (TG–DTG–DTA) were run in static air on a model OD-103 derivatograph of Hungarian origin (range 20–900 °C, Pt crucible, sample mass 500 mg, Al_2O_3 as reference, heating rate 5 K/min. The TG–DTG–DTA–MS measurements in argon (Ar 5.0) were run on a Setsys 16/18 derivatograph (Setaram) coupled with a Thermostar quadrupole mass spectrometer (range 20–700 °C, corund crucible, sample mass 17 mg, Al_2O_3 as reference, heating rate 5 K/min, flow rate of carrier gas 15 mL/min).

The DSC measurements were carried out in a model DSC 204 NETZSCH calorimeter (range 20–190 °C, Pan Al crucible, open, sample mass 4 mg, heating rate 5 K/min, flow rate 30 mL/min).

The course of thermal analysis was broken at points corresponding to the first step of decomposition and the residue in the crucible was quickly cooled. In the case of the product obtained in the inert atmosphere, the residue was cooled in the stream of argon. This enabled to analyze the residues at a strictly pre-determined step of decomposition. The analysis was carried out using the IR, far-IR, and Mössbauer spectroscopic techniques, as well as elemental analysis (C, H, N).

3. Results and discussion

3.1. Spectroscopic features of $[(C_4H_9)_4N][FeCl_4]$

The IR spectrum of the compound (KBr pellets, 16 scan, resolution at 4 cm^{-1}) is shown in Fig. 1.

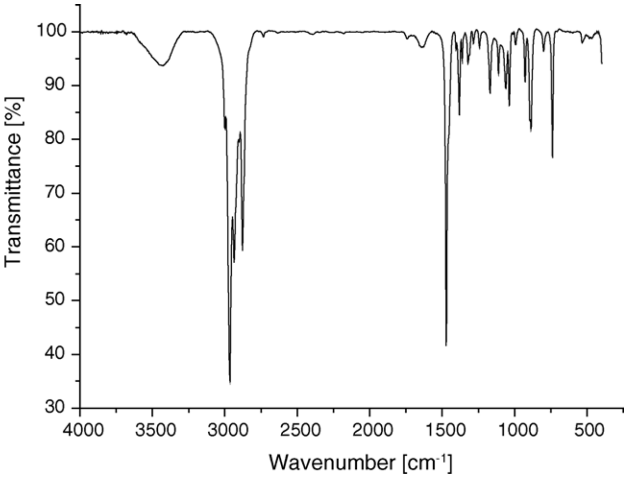

Fig. 1. The IR spectrum of $[(C_4H_9)_4N][FeCl_4]$.

To identify vibrational frequencies of Fe–Cl and Cl–Fe–Cl in the tetrachloroferrate(III) ion, the Raman spectra was recorded over the range 400–100 cm^{-1}. The frequencies: stretch $\nu_1(A_1)$, Fe–Cl, twist $\nu_2(E)$, Cl–Fe–Cl, stretch $\nu_3(F_2)$, Fe–Cl and twist $\nu_4(F_2)$, Cl–Fe–Cl for the $Fe(III)Cl_4^-$ ion, active in the Raman spectrum (Fig. 2), appear at ca. 330, 109, 378, and 134 cm^{-1}, respectively. On the other hand, in the far-IR spectrum (Fig. 6(1)) only the bands centered at 379 cm^{-1} ($\nu_3(F_2)$, Fe–Cl) and 137 cm^{-1} ($\nu_4(F_2)$, Cl–Fe–Cl) are active. These spectroscopic features are compatible with those obtained for other tetrachloroferrates [8] and reveal the presence of the ferric ion in a tetrahedral structure of chloride ions. The accumulated spectral evidence confirms also the complex structure of the salt.

3.2. Thermal analysis of $[(C_4H_9)_4N][FeCl_4]$

In Figs. 3 and 4 the results of thermal analysis of $[(C_4H_9)_4N][FeCl_4]$ are collected. The shapes of the TG

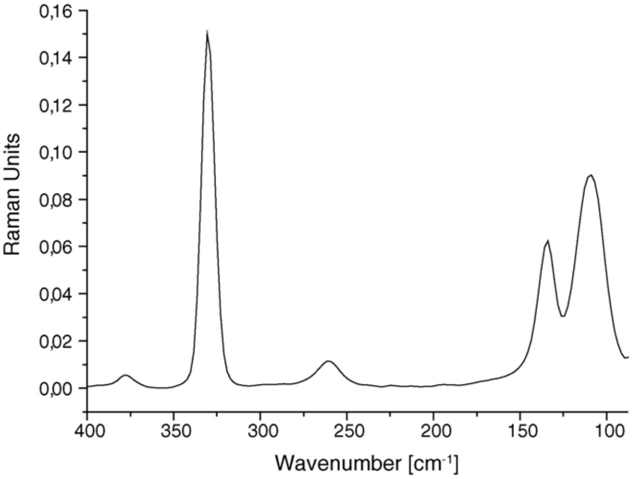

Fig. 2. The Raman spectrum of $[(C_4H_9)_4N][FeCl_4]$ taken over the range 400–100 cm^{-1}.

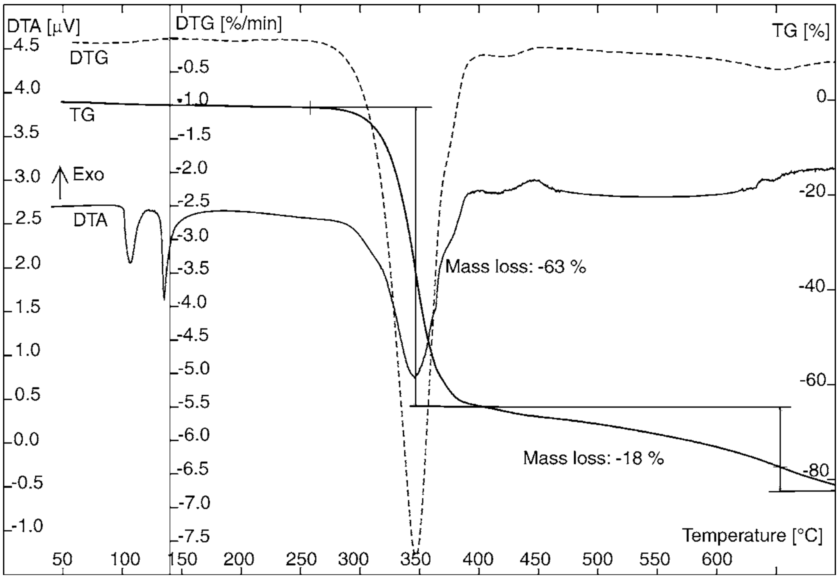

Fig. 3. TG, DTG and DTA curves of thermal decomposition of $[(C_4H_9)_4N][FeCl_4]$ in argon.

curves taken in the argon atmosphere (Fig. 3) and in static air (Fig. 4) are alike. First effects are seen at 110 and 135 °C (DTA), respectively, as two fairly sharp endothermic peaks accompanied by the lack of change in mass indicating the melting and phase transformation of the compound. There are two steps of thermal decomposition. The first one is rapid and the losses in mass are 65 and 63%, respectively, in static air (at ca. 420 °C) and argon (at ca. 410 °C). The rapid degradation suggests a dissociative nature of the decomposition proceeding without participation of oxygen. On the other hand, during the second step, oxidation of the residual carbon seems to predominate as shown by the exothermic event in the DTA curve during the run in the air atmosphere.

Unlike the run in argon, in the DTG trace taken in static air there are two minima (at 340 and 380 °C), and in the DTA trace there are two exothermic events at ca. 325 and 360 °C. This suggests that during the first step two successive degradation reactions take place. However, due to high rate of degradation these reactions cannot be unambiguously determined. The second step is much slower. In the static air it is slightly faster than in the argon atmosphere and is terminated at a by ca. 100 °C lower temperature. In the latter case all degradation steps are endothermic, whereas in static air all are exothermic owing to oxidation of the organic fragment of the compound.

Thermal degradation of the complex in both atmospheres is preceded by solid–solid and solid–liquid phase transforma-

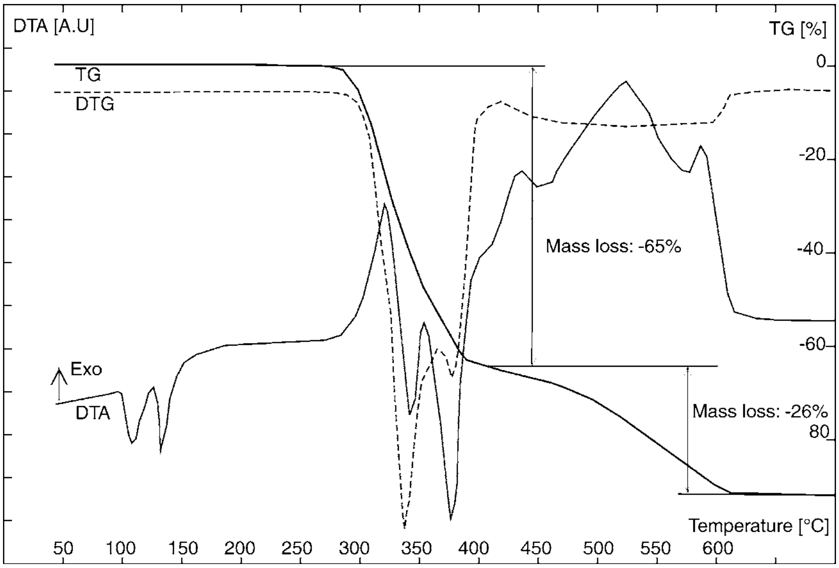

Fig. 4. TG, DTG and DTA curves of thermal decomposition of $[(C_4H_9)_4N][FeCl_4]$ in static air.

Table 1
Phase transition points and thermodynamic functions for $[(C_4H_9)_4N][FeCl_4]$

	Heating		Cooling	
Transition Point (°C)	106	136	117	68
ΔH (kJ/mol)	13.61	12.35	12.69	15.92
ΔS (J/mol K)	35.92	30.19	32.55	46.68

tions. The compound is stable up to 130 °C and then melts. The liquid phase persists up to ca. 255 °C and in this phase the complex undergoes degradation. That relatively high degradation point indicates a high stability of $[(C_4H_9)_4N][FeCl_4]$ in the melt.

As seen, the oven temperature has no effect on the phase transition points and the onset of degradation. Consequently, the degradation is determined by thermodynamic stability of the compound rather than by its reactivity with oxygen. Accurate phase transition points and inherent thermodynamic functions were determined from DSC measurements. The results are shown in Table 1.

The change in entropy, ΔS, calculated from equation: $\Delta S = \Delta H/T$, where T is the transition point. The DSC plot of the compound is presented in Fig. 5.

Upon cooling of the sample two phase transitions occur as well. However, the exothermic events are noted at lower temperatures (117 and 68 °C) than upon heating.

Gaseous degradation products of $[(C_4H_9)_4N][FeCl_4]$ in argon were analyzed using TG–MS. Owing to the complexity of processes taking place during the second step, only the first TG step was analyzed.

Already in the first step both the cation of the organic base and the tetrachloroferrate(III) ion undergo degradation. The terabutylammonium ion releases $(C_4H_9)_3N_{(g)}$ ($m/z = 100$, 142), $C_4H_9Cl_{(g)}$ ($m/z = 27$, 41, 56), $CH_3Cl_{(g)}$ ($m/z = 15$, 50, 52) and a very small amount of $Cl_{2(g)}$ ($m/z = 70$, 72) seems to form. A similar degradation pattern of the tetrabutylammonium ion has been noticed during the thermal degradation of plain tetrabutylammonium chloride in nitrogen [9] which gave $(C_4H_9)_3N_{(g)}$ and $C_4H_9Cl_{(g)}$.

A part of the gaseous products emitted in the argon atmosphere condensed on cold pieces of the apparatus to a greyish precipitate which contained 12.9% C, 21.6% H, 8.4% N and 54.8% Cl. This result shows that virtually the whole organic fragment of the compound was lost during the first step. The high chlorine content is indicative of the decay of the tetrachloroferrate(III) ion releasing the chloride ligands. It may also be due to some extent to sublimation of $FeCl_3$ at ca. 295 °C [10]. Both the elemental analysis and the IR spectra of the greyish precipitate suggest that it consists of a mixture of volatile products. On the other hand, both the colour of the precipitate and the broad 2750–2250 cm^{-1} IR band suggest that the gaseous products are likely to form aggregates consisting of two or more molecules. These speculations are consistent with the results of analysis of the gaseous products released during the first step.

The constituents of the solid residue of step I were identified by elemental analysis and far-IR spectroscopy. The results of elemental analysis reveal almost total volatilization of the organic fragment of the compound during the first step and the presence of a large amount of mineral constituents.

Some differences in spectral characteristics between the complex and its degradation products in argon and static air are presented in Fig. 6.

The bands due to Fe–Cl stretch and Cl–Fe–Cl twist in the spectrum of $[FeCl_4]^-$ occur at ca. 379 and 137 cm^{-1}. In the spectrum of the residue lefty in the argon atmosphere

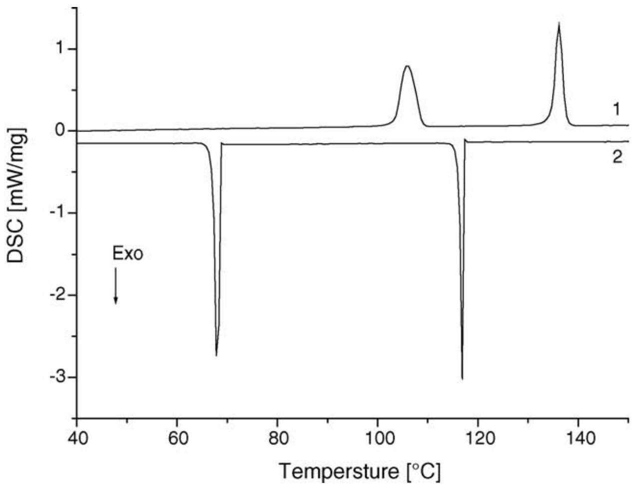

Fig. 5. The DSC plot for $[(C_4H_9)_4N][FeCl_4]$: (1) heating; (2) cooling.

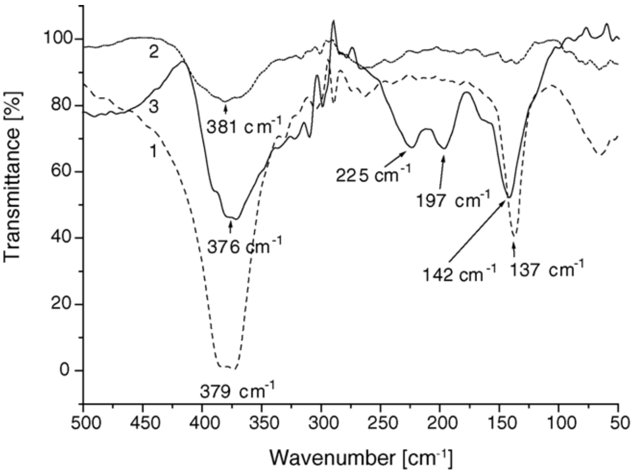

Fig. 6. Far-IR spectra of $[(C_4H_9)_4N][FeCl_4]$ (1) and of solid residue left after the first step of degradation in argon (410 °C) (2) and static air (420 °C) (3).

the 381 cm^{-1} band is narrower and markedly less intense, whereas the 137 cm^{-1} band is virtually missing. In the far-IR spectrum of the residue left in static air experiment, the band due to Fe–Cl stretch is less intense and displaced by a few cm^{-1} towards lower frequencies. Again, the band due to Cl–Fe–Cl twist is somewhat less intense as compared to that of unheated compound. Furthermore, two bands due to symmetric vibrations, of comparable intensities, emerge at ca. 225 and 197 cm^{-1}.

A closer inspection of the IR spectra leads to the following conclusions: (i) the quality of the product of the first degradation step depends on the oven temperature. However, it should be emphasized that the mass losses in both atmospheres are virtually identical; (ii) absorption bands due to stretching and bending vibrations became less intense probably due to their damping as a result of enhanced co-ordination of the ligands around the ferric ion; (iii) two new bands in the spectrum of the residue left in the static air experiment show that a lower-symmetry structure is preferred owing to partial or total inhibition of degeneration of the vibrations. In this case elimination of the degeneration may be due either to exchange of the chloride ligand or to formation of a new bond by the chlorine atom involved probably in a Fe–Cl–Fe bridge; (iv) the presence of only a single band in the spectrum of the precipitate formed in the argon atmosphere suggests that certain structures of higher symmetry around the ferric ion are preferred.

The colour of the residue formed in static air was non-uniform and consisted of a darker, somewhat glossy fraction (Fig. 6(3)), and a brighter one with a metallic luster.

The far-IR spectra of both fractions are shown in Fig. 7.

These spectra differ in the number and intensity of absorption bands. The differences may be due to the presence of iron in at least two co-ordination modifications.

Some additional information concerning the valence and spin states of iron in the starting sample and in the products of decomposition in static air and in argon may be drawn after analysis of Mössbauer spectra of studied samples.

The hyperfine interaction parameters, concluded from the resonance absorption spectra, mainly isomer shift δ, related to the s-elektron density at the nucleus and quadrupole splitting Δ, related to the electric field gradient give information on the local electronic state of the probe atom, here ^{57}Fe. In particular, iron(III) in high spin state (characterized by low δ and Δ values) and iron(II) in high spin state (characterized by high δ and Δ values) are easy to distinguish. Some dynamic and structural information may be obtained from the probability of resonance absorption given by recoil-free fraction *f*, that is proportional, for the thin absorbers, to the intensity of the resonance lines. The temperature dependence of the absorption line area may be used for the determination of local Debye temperature.

The Mössbauer spectra of samples as prepared and after heating are shown in Fig. 8 and the hyperfine parameters obtained after the numerical analysis are listed in Table 2. The spectrum of sample as prepared (Fig. 8a) has a shape of a slightly broadened single line resulting from the small quadrupole splitting of lattice origin. The value of δ equal to 0.21 mm/s is in agreement with the literature data [11] that confirms the presence of iron(III) in a form of $[FeCl_4]^-$ anion. In spectra of samples decomposed in air (Fig. 8b) and in argon

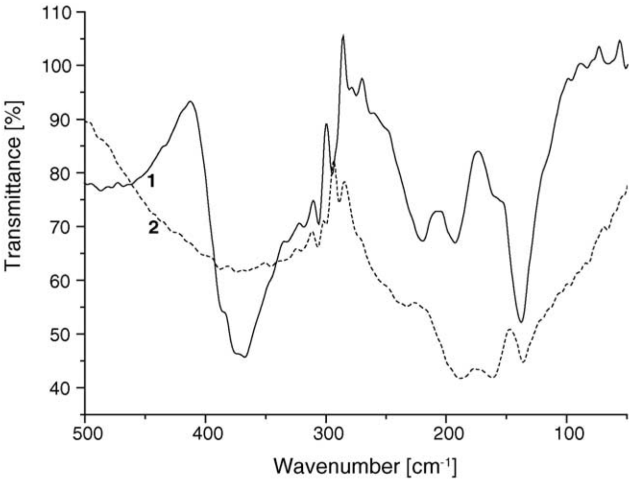

Fig. 7. The far-IR spectra of the darker (1) and brighter (2) fractions of the degradation product of $[(C_4H_9)_4N][FeCl_4]$ in static air (at 420 °C).

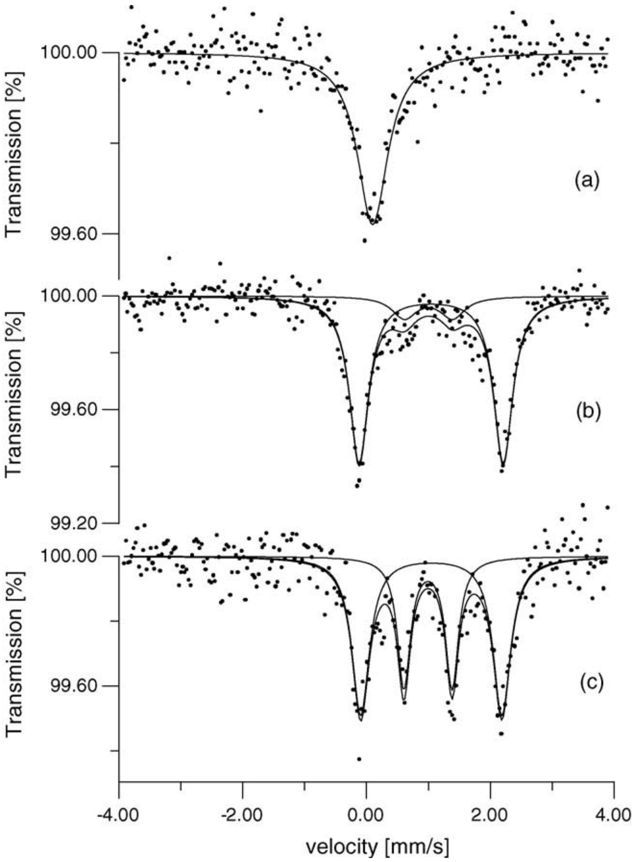

Fig. 8. Mössbauer spectra of $[(C_4H_9)_4N][FeCl_4]$ (a) and the products of its first degradation step in static air (b) and argon (c).

Table 2
Mössbauer parameters for $[(C_4H_9)_4N][FeCl_4]$ samples as prepared and after heating in air (420 °C)and in argon (410 °C)

Sample	*T* (K)	Fe^{3+}			Fe^{2+} (outer doublet)				Fe^{2+} (inner doublet)			
		δ (mm/s)	Γ (mm/s)	*A* (%)	δ (mm/s)	Δ (mm/s)	Γ (mm/s)	*A* (%)	δ (mm/s)	Δ (mm/s)	Γ (mm/s)	*A* (%)
As prepared	293	0.21 (1)	0.30 (2)	100								
Heated in air	293				1.15 (2)	2.32 (2)	0.19 (2)	85 (2)	1.10[a]	0.78[a]	0.24 (5)	15 (2)
Heated in Ar	293				1.15 (2)	2.28 (4)	0.17 (2)	62 (3)	1.10 (2)	0.78 (2)	0.13 (2)	38 (2)
	90				1.38 (2)	2.84 (2)	0.22 (2)	96 (1)	1.09 (4)	1.68 (8)	0.16 (6)	4.3 (8)
	220				1.21 (2)	2.50 (4)	0.18 (2)	100				
	293				1.16 (2)	2.32 (2)	0.16 (2)	100				

T: temperature of the measurement; Γ: absorber line width; δ: isomer shift versus room temperature α-Fe; A: relative contribution to the total spectrum; Δ: quadrupole splitting.

[a] Fixed parameter.

(Fig. 8c) two doublets–outer and inner, both corresponding to the Fe(II) states–are observed. It is worthwhile to note that after heating independently of the atmosphere the complete reduction forming Fe(II) has taken place. The contributions of both doublets to the total spectrum are different depending on the heating atmosphere.

The Mössbauer parameters (Table 2) of outer doublet are the same for samples decomposed in air and in argon. It suggests creation of the same form of Fe(II) in both samples. The quadrupole splitting Δ of inner doublet indicates the symmetry close to $[FeCl_4]^{2-}$ but isomer shift value is higher than found in the literature [12,13]. In order to characterize better the species attributed to this doublet the Mössbauer spectra of the sample heated in argon were recorded at low (90 and 220 K) and again room temperatures. The results are shown in Fig. 9 where in all spectra practically one doublet is present. Thus, some irreversible transformation has taken place leading to the formation of the same Fe(II) species which is attributed to outer doublet. Nevertheless at 90 K (Fig. 9a) the hardly visible inner doublet can be observed but its Mössbauer parameters are the same as assigned by Feist et al. [13,14] to more complicated structural units like $[Fe(II)Cl_5]^{3-}$. The reason of this transformation is not clear; it may be caused by cooling only or due to stay in vacuum in cryostat.

The temperature dependence of the outer doublet intensity was used to estimate the Debye temperature ($\Theta = \sim 200$ K) and consequently the recoil-free fraction ($f = 0.4$) value at room temperature for the Fe(II) form assigned to this doublet. The same procedure was applied to inner doublet taking into account Debye temperature of $[FeCl_4]^{2-}$ estimated by Edwards et al. [12] to be of the order of 100 K which leads to $f = 0.07$ value at room temperature. Because the intensity of the resonance line is proportional to product *fn*, where *n* denotes number of Fe^{2+} ions in considered state, one can obtained the proper content of determined phase. Thus, in the sample heated in air the ratio of both Fe(II) species is about 50%:50% This result is consistent with the IR spectra where for product decomposed in air two different iron coordinations are recognised. In the sample heated in argon, in spite of apparently equal intensities of both doublets, the iron state attributed to inner doublet dominates and the ratio of two component areas is estimated as 80%:20%.

The Debye temperature of ∼200 K calculated for iron state ascribed to outer doublet is much higher than for inner one (∼100 K) that is evidence of stronger Fe(II) bonds in the former case and may be related to the increase of the iron coordination number. In addition, the weak temperature

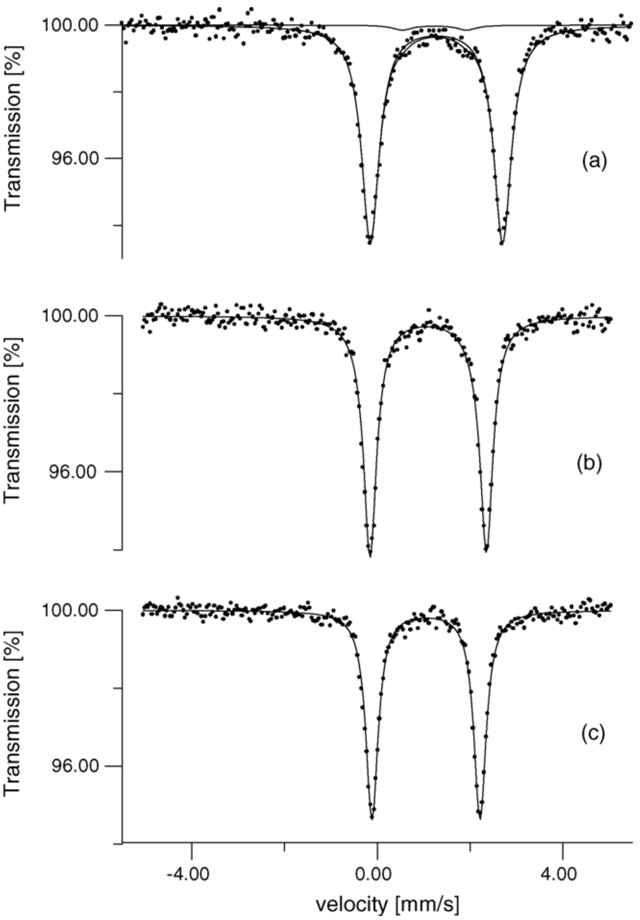

Fig. 9. Mössbauer spectra of the product of the first degradation step in argon taken at 90 K (a); 220 K (b), and again at 293 K (c).

dependence of Δ suggests strong ligand field around the iron atom and may be associated with the low symmetry environment of Fe(II) species ascribed to outer doublet.

4. Conclusions

The new compound has a structure of a complex salt with tetrahedral arrangement of the chloride ions around the iron atom.

The shapes of the TG traces taken in static air and in argon are similar. In both atmospheres the degradation occurs in two steps preceded by solid–solid and solid–liquid phase transformations. In the melt the compound is fairly stable. Its degradation occurs at a temperature by ca. 100 °C higher than its melting point. Already in the first step, both the tetrabutylammonium and the tetrachloroferrate(III) ions undergo degradation. The chloride ions are released as CH_3Cl, C_4H_9Cl and Cl_2. The presence of chlorine in the volatile products may be due to reduction of Fe(III) to Fe(II) with simultaneous oxidation of the chloride ions.

This hypothesis has subsequently been supported by inspection of the Mössbauer spectra of both products of the first step of degradation, which revealed the presence of iron(II) only. The composition of degradation products of the first step depends on the oven temperature. However, the oven atmosphere has no influence on mass losses. This shows that the degradation of the compound is determined by its thermodynamic stability rather than its reactivity with oxygen.

During experiments in static air a structure of lower symmetry is preferred owing to enhanced co-ordination around the iron atom, while in argon a structure of higher symmetry dominates. Furthermore, far-IR spectra of the residue left after the first step in static air experiment suggest that this residue contains at least two co-ordination modifications of iron.

This suggestion is supported by Mössbauer spectra that reveal iron(II) in two different chemical environments present in comparative amounts (about 50%:50%). On the other hand in the degradation product obtained in argon atmosphere one of the two coordination modifications dominates. It is more thermodynamically stable and characterized by higher symmetry. The ratio of both iron forms in this degradation product was estimated to ca. 80%:20%.

Further study aimed at in-deep explanation of the mechanism of the thermal processes is under way.

Acknowledgement

This research was supported by the Polish State Committee for Scientific Research under Grant DS/8230-4-0088-5.

References

[1] J.A. Zora, K.R. Seddon, P.B. Hichcock, C.B. Lowe, D.P. Shum, R.L. Carlin, Inorg. Chem. 29 (1990) 3302–3308.
[2] C.B. Lowe, R.L. Carlin, A.J. Schultz, C.-K. Loong, Inorg. Chem. 29 (1990) 3308–3315.
[3] A.P. Ginsberg, M.B. Robin, Inorg. Chem. 2 (1963) 817–822.
[4] J.S. Avery, C.D. Burbridge, D.M.L. Goodgame, Spectrochim. Acta 24A (1968) 1721–1726.
[5] K.D. Butcher, S.V. Didziulis, B. Briat, E.I. Solomon, J. Am. Chem. Soc. 112 (1990) 2231–2242.
[6] Z. Warnke, G. Wawrzyniak, D. Wyrzykowski, J. Kosmalski, Polish J. Chem. 75 (2001) 759–763.
[7] Z. Warnke, D. Wyrzykowski, G. Wawrzyniak, Polish J. Chem. 77 (2003) 1121–1129.
[8] K. Nakamoto, Infrared and Raman Spectra of Inorganic and Coordination Compound, Wiley, New York, 1986.
[9] J. Błażejowski, E. Kowalewska, Thermochim. Acta 105 (1986) 257–285.
[10] W.W. Pieczkowski, N.I. Worobiew, Ż. Nieorg, Chim. 9 (1964) 12–19.
[11] C.A. Clausen III, M.L. Good, Inorg. Chem. 9 (1970) 220–223.
[12] P.R. Edwards, C.E. Johnson, R.J.P. Williams, J. Chem. Phys. 47 (19672074).
[13] M. Feist, S.I. Troyanov, H. Mehner, K. Witke, E. Kemnitz, Z. Anorg. Allg. Chem. 625 (1999) 141–146.
[14] M. Feist, R. Kunze, D. Neubert, K. Witke, H. Mehner, E. Kemnitz, Thermochim. Acta 361 (2000) 53–60.